

EXTREME ULTRAVIOLET OBSERVATIONS OF HOT WHITE DWARFS

Stuart Bowyer

Department of Astronomy
University of California, Berkeley

I. Introduction

The term extreme ultraviolet (EUV or XUV) is employed in upper atmosphere physics and in solar work where it usually denotes the wavelength band between 100 and 1000 Å. Since thermal emission with $30,000 \lesssim T \lesssim 300,000$ K peaks in this band, it might be expected that studies at these wavelengths would be especially useful for objects with effective temperatures in this range. In fact, few such studies have been carried out. The reason for this anomaly is that very few EUV studies have been made at all, particularly because of unreasonably pessimistic estimates of the opacity of the interstellar medium and partially because of instrumental difficulties encountered at these wavelengths. The first search for extreme ultraviolet emitting objects was carried out in 1975 with instrumentation on the Apollo spacecraft in the Apollo-Soyuz mission. Four of approximately thirty preselected objects were detected with this instrumentation. The objects detected unquestionably are more a reflection of the prejudices of the investigators than they are a sampling of the contents of the universe. Nonetheless, two of the four objects detected were hot white dwarfs: HZ 43 and Feige 24. In addition, upper limits which turned out to be extremely useful were obtained on the Sirius A/B system. These results, plus more recent results obtained on hot white dwarfs will be discussed in this review.

II. Interstellar Absorption

Historically, absorption at EUV wavelengths due to the interstellar medium (ISM) was considered to be so severe that no measurements would be possible at these wavelengths. The attenuation to a particular source is the summed effect of all the elements in the intervening ISM and is usually expressed as $\exp(-L n_H \sigma_{\text{eff}})$ where L is the path length, n_H is the average hydrogen density, and σ_{eff} is the effective absorption cross section for all the elements in the ISM normalized to n_H (since $N_H = L n_H$ is often the experimentally observed parameter). Using an average value of $n_H \sim 1 \text{ cm}^{-3}$ led to the conclusion that no useful EUV observations could be made. However, evidence has been steadily accumulating which indicates that within at least 100 pc of the Sun the ISM is considerably below this value. A tabulation of the current observational data on this parameter has been assembled by Cash, Bowyer, and Lampton (1979) and is reproduced here as Table I. (The reader is referred to Cash et al. for the relevant references).

TABLE I

<u>Star</u>	<u>Distance (pc)</u>	<u>$n_{\text{HI}} (\text{cm}^{-3})$</u>	<u>Reference for Column Density of HI</u>
Sun	-	.1	Freeman et al. (1979)
α Cen	1.34	.06 - .30	McClintock et al. (1978)
ϵ Eri	3.3	.06 - .20	McClintock et al. (1978)
ϵ Ind	3.4	~.1	McClintock et al. (1978)
α CMi	3.5	.09 - .13	Anderson et al. (1978)
β Gem	10.8	.02 - .15	McClintock et al. (1975)
α Boo	11.1	.02 - .15	McClintock et al. (1975)
α Aur	14	.04 - .05	McClintock et al. (1978)
α Tau	21	.02 - .15	McClintock et al. (1975)
α Leo	22	.02 .01	Rogerson et al. (1973) Kondo et al. (1978)
λ And	26	.03 - .08	Baliunas and Dupree (1979)
α Eri	28	.07	Rogerson et al. (1973)
α Gru	29	.09 - .18 .18	York (1976) Kondo et al. (1978)
HR 1099	33	.003 - .007	Anderson & Weiler (1978)
η UMa	42	0.005	York (1976)
G191 - B2B	47	>.03	Cash et al. (1979)
σ Sgr	57	<0.17	Bohlin et al. (1978)
HZ 43	62	<0.013	Auer and Shipman (1977)
α Pav	63	<0.1	Bohlin (1975)
β Cen	81	0.13	Bohlin et al. (1978)
β Lib	83	0.06 - 0.13	York (1976)
ζ Cen	83	<0.39	Bohlin et al. (1978)
α Vir	87	0.037	Bohlin et al. (1978)
Foige 24	90	.02	Cash et al. (1979)
λ Sco	100	<0.078	Bohlin et al. (1978)

The interstellar density within 100 AU of the Sun has been measured by observations of backscattered solar HI λ 1216 and HeI λ 584 (Fahr, 1974; Freeman et al., 1979 and references therein). Measurements of interstellar absorption lines in the ultraviolet spectra of nearby stars have been made by both the OAO-2 and Copernicus satellites, but because of their higher accuracy, only Copernicus measurements are included in this Table. All the column densities out to 21 pc plus the column density for HR 1099 were obtained through observation of the interstellar absorption core in the chromospheric H α λ 1216 line. In the other stars between 22 and 42 pc the interstellar NI column density was measured and with assumptions about the nitrogen abundance these were converted to hydrogen densities. In the more distant stars, the H α absorption was measured against the stellar continuum to obtain n_{HI} except for the white dwarfs where n_{HI} is obtained from the EUV data.

In Figure 1, the measured column densities from Table I are plotted as a function of distance. Some of the upper limits in the table are sufficiently poor to be of little direct interest and hence were not plotted. The dashed line represents a simple linear regression of column density versus distance with the line slope providing an average hydrogen density of $\langle n_{\text{H}} \rangle = .07 \text{ cm}^{-3}$. While this value is more than an order of magnitude below the canonical average of 1 atom cm^{-3} , even more

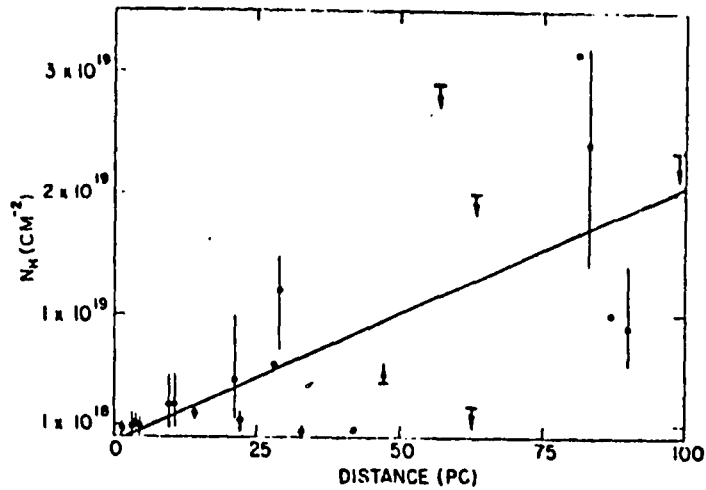


Fig. 1 - Column densities for stars within 100 parsecs of the Sun plotted against distance (After Cash *et al.*, 1979).

significant is that out to 25 pc there is no obvious increase of column density with distance. In addition there is obvious patchiness at all larger distances. Cash *et al.* argue from these data that typically three clouds of size 5 to 15 pc and $N_H \sim 5 \times 10^{18} \text{ cm}^{-2}$ are to be expected in a random line of sight to 100 pc. While this is at best a preliminary estimate, it is remarkably similar to predictions by McKee and Ostriker (1977). These authors have developed a multiphase model of the ISM with clouds of diameter 4 pc and $N_H \sim 2 \times 10^{18} \text{ cm}^{-2}$, shielded by partially ionized gas at temperatures near 8000 K, and embedded in a network of gas at 10^5 to 10^6 K which is produced by shocks due to supernovae.

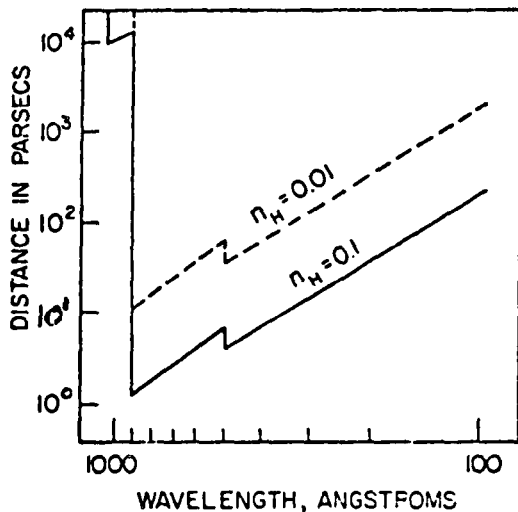


Fig. 2 - Distance to which attenuation is 90% as a function of wavelength. Upper curve is for an interstellar hydrogen density of 0.01; lower curve is for a hydrogen density of 0.1.

From an observation viewpoint alone, the data in Table I indicate that within 100 pc n_H is typically in the range of .01 to 0.1 atoms cm^{-3} . Folding these values with the EUV effective cross section of Cruddace *et al.* (1974) we obtain the results shown in Figure 2 where we have plotted the 90% attenuation distance as a function of wavelength. We see we have fair chance of observing sources at wavelengths as long as 300 Å at distances as far as 100 pc. Since there are at least 100,000 stellar objects within this distance, we have some reasonable hope that a subset of these exist which are emitting at EUV wavelengths. Certainly a substantial number of white dwarfs exist within this volume. It may even be possible

to observe extragalactic objects at 100 to 200 Å in selected directions near the galactic poles, and stars within 10 pc of the Sun may be observable over the entire EUV band.

III. Instrumentation

A substantial amount of the data reported here were obtained with the EUV telescope flown on the Apollo-Soyuz mission. It may well be profitable to summarize that instrumentation here, and provide some general remarks on this type of instrumentation which will be useful for a critical evaluation of the data that is presented later.

The Apollo-Soyuz extreme ultraviolet telescope consisted of a nested set of parabolic grazing-incidence reflectors having an aperture of 37cm, a six position filter wheel, and a channel electron multiplier photon counter. The filter wheel rotated continually at 10 rpm to give nearly continuous coverage of stellar fluxes in five wavelength bands; the sixth opaque position permitted the detector dark count rate to be monitored. The instrument's field of view was circular with a diameter of 2.5°. Count rates were telemetered each 0.1 sec, along with auxiliary information. Preflight laboratory calibration was conducted using a variety of wavelengths between 44 Å and 2650 Å. Absolute photon fluxes were determined with NBS vacuum-photodiode standards longward of 200 Å, and with primary standard propane counters at shorter wavelengths.

The telescope was not capable of imaging and hence operated only as a flux collector. This limited the sensitivity of the instrument to those sources which were more intense than the summed background flux from the entire field of view of the telescope. Since there are substantial daytime background fluxes at 304 and 584 Å which cannot be completely discriminated against, this effectively required that all observations be made in the Earth's shadowcone. Even in spacecraft darkness, substantial background fluxes at He II 304, He I 584, and H I 1216 Å can be present.

The quantum efficiency of the channel electron multiplier used in this telescope is shown in the upper panel of Figure 3 (Mack, Paresce, and Bowyer, 1976). As can be seen, it has a substantial response at wavelengths other than the EUV. The short wavelength response of an EUV telescope can be rigorously controlled by appropriately choosing the grazing angles of the mirrors. Eliminating the unwanted response longward of 912 Å is more difficult and is achieved by insuring the thin metallic films used as bandpass filters have no response outside their primary transmission band. While this approach is effective in principal, nature does not provide a large selection of suitable films. The best choices available at the time of the Apollo Soyuz flight were parylene N (an organic carbon film), beryllium with carbon, aluminum with carbon, and tin. The effective area of the telescope at each bandpass with all instrument parameters included is shown in the lower panel of Figure 3. It should be noted that these films are typically only hundreds to a few thousand angstroms thick. They are both quite fragile and easily degraded. One common form of degradation is the formation of pinholes which has the obvious effect

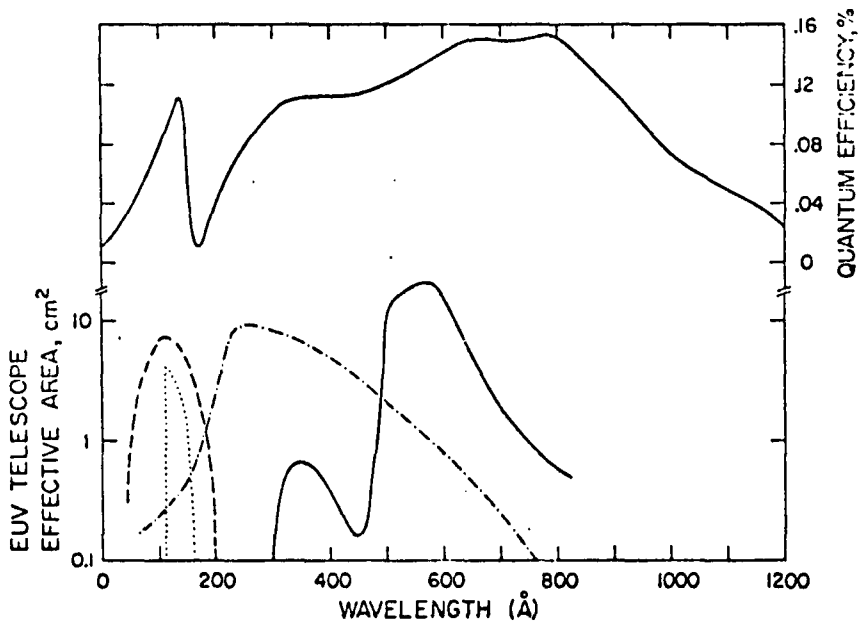


Fig. 3 - Top Panel: Graph of Quantum Efficiency vs. wavelength for a channel electron multiplier. Lower Panel: Graph of effective area of the Apollo Soyuz EUV Telescope for each EUV filter. Dashes = carbon film; dots = Beryllium plus carbon film; dot dash = Aluminum plus carbon film; solid = Tin film.

of making the device sensitive to the entire EUV band as well as part of the far UV band.

In the case of the Berkeley instrument on the Apollo-Soyuz flight, a variety of inflight checks were carried out which verified the integrity of the filters against pinholes. However, since the payload was not recovered, the constancy of the response of the telescope at each bandpass could not be verified. In fact, because of the existence of independent and time coincident measurements of the 584 Å background flux, we were able to determine that the tin filter bandpass of our telescope decreased in sensitivity by a factor of two between our final calibration and flight operations (Freeman *et al.*, 1979). It will probably be some time before EUV measurements reach the level of accuracy and consistency of ground based optical astronomy.

IV. HZ 43

The hot white dwarf HZ 43 (Humason and Zwicky, 1947; =EG 98, Eggen and Greenstein, 1965; =L1409-4, Luyten, 1949; =FB127, Greenstein and Sargent, 1974) was chosen as an object for investigation on the Apollo-Soyuz mission on a number of grounds. Shipman (1972) had derived $T_{\text{eff}} \geq 50,000$ K from the slope of the optical continuum. A very soft X-ray source in Coma was first reported by Hearn *et al.* (1976) and the possibility of an identification with HZ 43 was raised. Our group also detected this source as a soft X-ray object (Margon *et al.*, 1976c) and found that a black body model with any $T_{\text{eff}} < 600,000$ K fit the data. Perhaps more important was that no long wavelength cut-off due to interstellar absorption was found. Taken together, these

observations were highly suggestive that HZ 43 would be an EUV source and that the interstellar medium might be sufficiently low to allow significant data to be obtained on this object.

The HZ 43 system was observed as part of the planned schedule for the Apollo-Soyuz mission and was detected in three of the EUV band-passes, making the object the first extrasolar object detected in the extreme ultraviolet (Lampton *et al.*, 1976). On the zero order assumption that the source was a black body radiator, these data restrict the temperature of the star to $40,000 \leq T_{\text{eff}} \leq 140,000$ K.

Margon *et al.* (1976b) obtained extensive optical data on the two stars that make up the HZ 43 system. The stars were classified as DA wk and dM3.5e. A distance of 65 ± 15 pc to the system was obtained independently by spectroscopic and trigonometric parallaxes. Combining the EUV data and the optical data with an assumption that the white dwarf radiates as a black body, these authors obtained a temperature of $110,000 \pm 10,000$ K for this star.

Auer and Shipman (1977) have derived a self-consistent model atmosphere for HZ 43 using Auer-Mihalas and ATLAS model atmospheres. In this analysis the intensity in the visible and the distance fixed the radius of the star, ultraviolet observations gave the interstellar

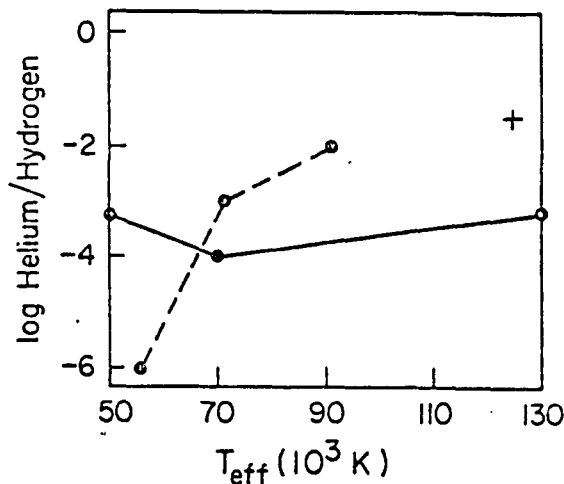


Fig. 4 - The photospheric helium to hydrogen abundance ratio for HZ 43 as a function of temperature of the star. The dashed line is the locus of points fitting the visible continuum and the EUV observations. Regions above the solid line would produce a detectable He λ 4686 line which is not observed. Cross is a high helium model by Durisen *et al.* (1976). (After Auer and Shipman, 1977).

reddening, the longest EUV detection fixed the interstellar hydrogen density, and the two shorter EUV wavelength detections gave the effective temperature as a function of helium abundance. Upper limits on the helium abundance were obtained from the observational upper limit of 120 mÅ to the equivalent width of He II 4686. The result of this analysis is shown in Figure 4. Also included in this figure is a high helium abundance model computed by Durisen *et al.* (1976). Auer and Shipman conclude that acceptable models for HZ 43A range in temperature from 55 to 70,000 K.

Greenstein and Oke (1979) have obtained ultraviolet spectra of HZ 43 with the IUE spacecraft. Their results are reproduced in Figure 5. Although a statistical criterion is not provided, these authors state the 60,000 K model atmosphere fits better than the 40,000 or the 50,000 K models.

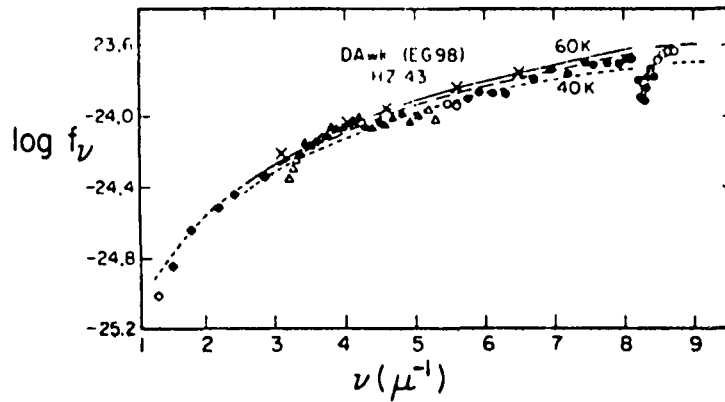


Fig. 5 - Far ultraviolet spectra of HZ 43 from IUE. The three lines are fits to the data of 40, 50, and 60,000 K. (After Greenstein and Oke, 1979).

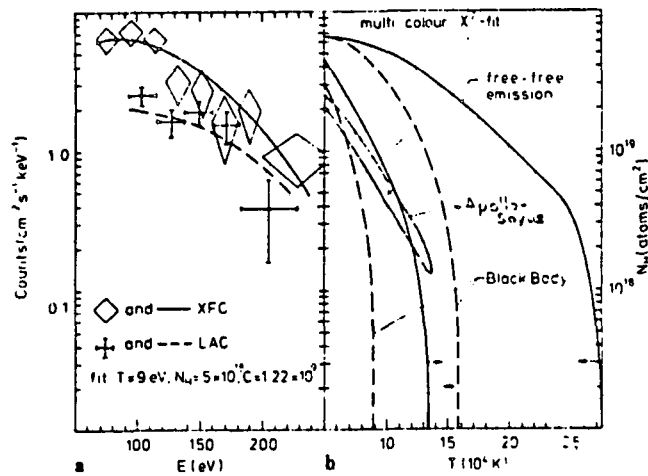


Fig. 6 - Left Panel: soft X-ray and EUV data on HZ 43 (after Bleeker *et al.*, 1978). The diamonds and crosses are the data from two counters with different thickness windows. Right Panel: 90% isoprobability contours for black body and coronal models. The cross is the particular black body model displayed with the data in the left panel. The curve marked Apollo-Soyuz is the 90% isoprobability contour for the Apollo-Soyuz EUV data for a black body model.

Wesselius and Koester (1978) obtained ultraviolet photometry of HZ 43 with the ANS spacecraft. These data, in combination with optical data and modeling of the H α and H δ lines lead these authors to conclude that the effective temperature of HZ 43 is in the range 60,000 \pm 5000 K.

Bleeker *et al.* (1978) have observed HZ 43 over the wavelength band between 44 and 170 Å with proportional counters. The data obtained are shown in Figure 6, left panel. A word of caution should be made about these data. Because of intrinsic energy smearing of X-ray proportional counters, the data points shown are not independent. For example, at 44 Å $\Delta E/E$ is about 100% with the spreading getting rapidly worse with decreasing energy. Hence, one can obtain one or, at most, two independent data points longward of 44 Å. The use of two different window thicknesses will provide an additional independent datum, of course. Because of the large energy smearing, the range of fits allowed by low energy proportional counter data is typically quite large (Figure 6, right panel). Any models with parameters within these contour limits can be considered to fit the data equally well at the same confidence level. For example, an extrapolation of the typical fit specified in this figure overshoots the peak EUV flux by a factor of at least three. However, an equally valid fit with a slightly larger temperature extrapolates through the EUV flux. Whether a particular data set is compatible with a given model can only be determined by detailed model fitting. In the right panel of Fig. 6, we have indicated the black body model parameters compatible with the Apollo-Soyuz EUV results. The area of overlap shows the range of parameters acceptable to both sets of data. For this particular model the range of overlap includes the most probably hydrogen column density within the 90% confidence level contours of both data sets.

Heise and Huizenga (1979) have attempted to fit a detailed model atmosphere to the entire data set used by Auer and Shipman with the addition of the soft X-ray data of Bleeker *et al.* They found they were unable to obtain an acceptable fit with standard models and investigated the effect of a gradient in helium density in the surface layers of the star. They have concluded that a surface layer of hydrogen with $\text{He}/\text{H} \lesssim 10^{-5}$ with mass of the order of one gm/cm^2 overlaying a helium rich lower layer with $\text{He}/\text{H} \gtrsim 10^{-1}$ is indicated by the data. Analyses by Koester (1976), Vauclair and Reisse (1977), and Fontaine and Michaud (1979), indicate that such a hydrogen layer would indeed remain stable against mixing. Independent of whether the existing data demand this configuration for HZ 43, Heise and Huizenga have raised the fascinating possibility that EUV and soft X-ray data may eventually provide a probe of the outer layers of a white dwarf.

We have recently developed an astronomical EUV spectrometer at Berkeley. The instrument is described in some detail by Malina *et al.* (1979); in brief, it consists of a Woltjer-Schwarzschild Type II telescope, a novel stigmatic Type III concave holographic grating, and a microchannel plate detector with a two-dimensional resistive anode readout. The instrument was flown on a sounding rocket and a spectrum of HZ 43 was obtained with 15 Å resolution over wavelengths from 200 to 500 Å. No emission or absorption features were observed but the He II Lyman edge was detected with decrement $F_\lambda(230 \text{ Å})/F_\lambda(220 \text{ Å}) = .51 \pm .13$ (Malina and Bowyer, 1979).

These data are displayed in Figure 7. Also shown on this figure are selected optical and UV fluxes and the EUV broadband flux from the Apollo-Soyuz measurement. The upper limit in the 500 to 800 Å band

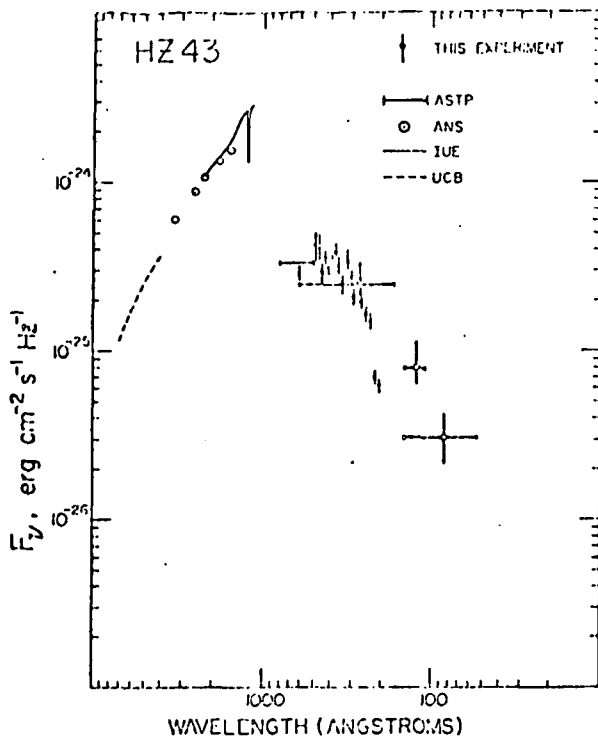


Fig. 7 - The spectrum of HZ 43. The EUV spectrometer data are shown as solid vertical lines. The Apollo-Soyuz broadband EUV measurements are shown as solid crosses. The solid line in the UV is from Greenstein and Oke (1979), and the circles are from Wesselius and Koester (1978). The dashed line in the optical is from Margon *et al.* (1976).

Apollo-Soyuz mission. A strong flux was found in the 170 to 620 Å band but no discernible flux was observed in the other filter bands (Margon *et al.*, 1976a). The resultant EUV energy distribution is radically different than HZ 43. The inferred fluxes and upper limits are shown in Figure 9 along with optical (Oke, 1974), and far ultraviolet (Holm, 1976) data. The solid line shown in Figure 9 is that of a pure hydrogen model atmosphere developed by Margon *et al.* with $\log g = 8$ and $T = 60,000$ K. The fit is obviously poor. Nonetheless, the star must be hotter than 50,000 K to provide sufficient 170 to 620 Å flux. While all these models hotter than 30,000 K had more 100 Å flux than was observed, the addition of a small amount of helium will reduce the flux in this band and may provide a satisfactory fit to the data.

On the basis of the ultraviolet data alone, Holm (1976) concluded that the star had a temperature in the range 55,000 to 70,000 K. Wesselius and Koester (1978) obtained a temperature of 63,000 K from modeling a combination of ANS ultraviolet data and optical data. Their model is not consistent with the EUV measurement, but with an admixture of helium with $n(\text{He})/n(\text{H}) = 10^{-3}$ a suitable fit is obtained in both the

has been increased to account for the change in sensitivity of this filter discussed earlier herein and more fully in Freeman *et al.* (1979). The discrepancy of perhaps a factor of two between the spectrometer measurement and the Apollo-Soyuz measurement at 120 to 160 Å should definitely be resolved in favor of the spectrometer data as this instrument was recovered and in a post-flight calibration, showed no change in sensitivity from the prelaunch values.

Heise and Huizenga (1979) have computed a grid of the He II ($\lambda 228$) Lyman jump as a function of effective temperature and helium abundance for uniform models with $g = 18^8 \text{ cm s}^{-2}$. In Figure 8 we have plotted our results on this grid for a range of temperatures; for $T = 60,000$ K this implies $1 \times 10^{-5} < n(\text{He})/n(\text{H}) < 3 \times 10^{-5}$.

V. Feige 24

The white dwarf Feige 24 (Feige 1958; =EG20, Eggen and Greenstein, 1965; =FB24, Greenstein and Sargent, 1974) was detected as an EUV source on the

Fig. 8 - Grid of photospheric helium abundance vs. temperature for uniform abundance atmosphere with $g = 10^8 \text{ cm s}^{-2}$. Diagonal lines delineate the size of the He II ($\lambda 228$) decrement. The allowed region for HZ 43 (shaded) is bounded by the temperature limits of Auer and Shipman (1977) and the decrement limits of Malina and Bowyer (1979).

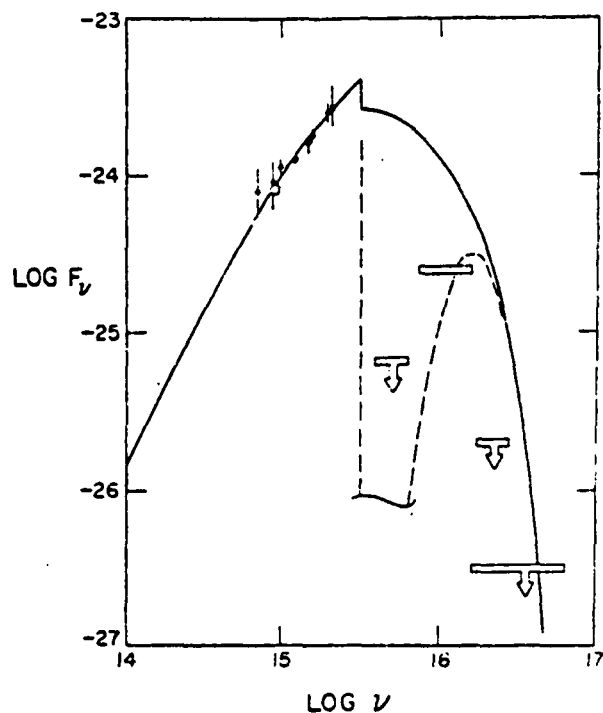
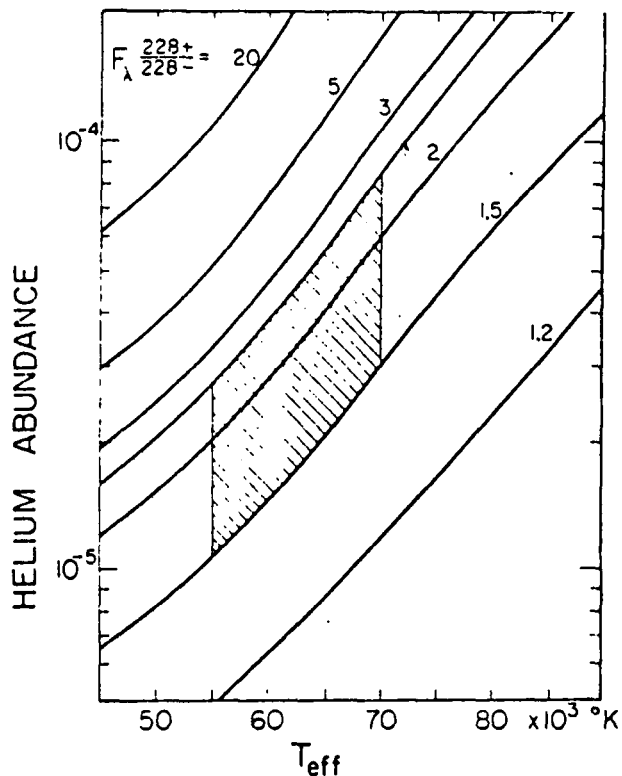


Fig. 9 - Spectral energy distribution of Feige 24, in $\text{erg cm}^{-2} \text{ sec}^{-1} \text{ Hz}^{-1}$. Boxes: EUV data, Margon *et al.*, dots: UV data, Holm, 1976; circle, Oke, 1974. Also shown is one model having $T_{\text{eff}} = 60,000 \text{ K}$ and $\log g = 8$, without (solid line) and with (dashed line) interstellar attenuation. (Margon *et al.*, 1976).

UV and the EUV. An analysis using the entire data set seems warranted. In this regard, Cash *et al.* (1979) have obtained an upper limit on the EUV flux from Feige 24 of $0.2 \text{ photons cm}^2 \text{ sec}^{-1} \text{ eV}^{-1}$ with an instrument with peak response at 300 \AA and with most of the sensitivity between 250 and 350 \AA . This indicates most of the observed EUV flux must lie between 170 and 280 \AA . Data from the soft X-ray detector on the HEAO-1 spacecraft show that in the 44 to 80 \AA band, Feige 24 is $< 1/30$ of the intensity of HZ 43.

In the optical band, Feige 24 is a remarkable object. Its spectrum contains sharp hydrogen Balmer and Ca II emission lines superimposed upon the broad Balmer absorption of a normal DA white dwarf (Eggen and Greenstein, 1965). This emission led these authors to propose that the system might be similar to an old nova. Direct evidence that the system was binary was given by Oke (1974), whose spectrophotometric measurements indicated the presence of a red component. With high resolution spectrophotometry, Liebert and Margon (1977) were able to classify the red component as M1 to M2V on the basis of the TiO band strengths. This led to a distance estimate of $\sim 90 \text{ pc}$. Liebert and Margon also found the intensity of the emission lines to be variable on timescales of $\sim 1 \text{ day}$, but to be essentially constant on shorter timescales. Thorstensen *et al.* (1978) obtained Coudé spectra of the system and found that the radial velocities of the lines varied regularly with a period of 4.23 days. They concluded that the emission lines were the result of EUV radiation from the white dwarf being reprocessed in the atmosphere of the red dwarf. The intensity variation of the lines was concluded to be the result of observing differing amounts of the heated hemisphere. By modeling this effect, they were able to determine the mass of the white dwarf to $.46 \leq M \leq 1.24 M_{\odot}$.

VI. Feige 4

Sagdeev, Kurt and Bertaux (1979) have reported the possible detection of an EUV source emitting in the 500 to 700 \AA band from a joint Russian-French experiment flown on the PROGNOZ-6 spacecraft. Bertaux (private communication) reports that the detection was with a 0.6 cm^2 channel electron multiplier with a thin tin filter. The signal observed was not a background feature and is best described by a point source. A signal of $\sim 4 \text{ counts s}^{-1}$ above background was seen on each of a number of sequential scans through the source region. Sagdeev *et al.* have suggested the hot white dwarf Feige 4 as a possible optical counterpart. A complicating factor is the existence of a B21V star, γ Pegasus, close to the position of Feige 4. This star is an obvious source of far UV emission and this point should be considered in connection with the possible degradation of thin films noted earlier. A detailed analysis is underway regarding this observation.

Feige 4 (=LB433 =EG3) is a DB white dwarf; photometry reported by Eggen and Greenstein (1965) gives $B = 15.22$, $B-V = -0.12$ and $U-B = -0.97$ which is similar to values recently remeasured by Liebert *et al.* (1979). These colors are not atypical for this type star. Using two circumstantial arguments, Eggen and Greenstein suggest that M_v is in the range 11 to 13 which would put this star 30 to 70 pc. away.

VII. Sirius B

The DA white dwarf Sirius B is unquestionably the most studied of all the white dwarfs. Unfortunately, the temperature of this star is difficult to determine. Greenstein, Oke, and Shipman (1971) found $32,000 \pm 1,000$ K from the H α line profile and model atmosphere calculations; Savedoff *et al.* (1976) found $27,000 \pm 6,000$ K from far ultraviolet measurements obtained with the Copernicus satellite, and Rakos and Havlen (1977) found 32,000 K from UBV and uvby photometry.

The discovery of soft X-rays from the Sirius system (Mewe *et al.*, 1975) was extremely surprising. Several models were developed to explain this flux. Mullan (1976) suggested that Sirius A may have a corona similar to the Sun, which by simple scaling can produce the observed flux. This suggestion has been criticized by several workers on the grounds that the physics of coronae are unquestionably more complex than this. Hearn and Mewe (1976) argued that the X-rays were produced in a corona around Sirius B. Several authors argued that this model, which was based on a convective helium envelope, was inappropriate for DA stars such as Sirius B. However, Lampton and Mewe (1979) developed a detailed model which showed that with a hydrogen surface layer overlaying a helium rich atmosphere, convective heating is marginally capable of producing a corona for Sirius B. The third possibility was advanced by Shipman (1976) who showed that if the effective temperature of the hydrogen atmosphere is above 32,000 K, the photosphere will emit sufficient soft X-rays to explain the observations. Because of its elegance and because of the strong consensus that the temperature of Sirius B was 32,000 K, this model seemed quite compelling. Shipman *et al.* (1977) also showed that this photospheric model was consistent with upper limits on the EUV flux from Sirius B obtained on the Apollo-Soyuz mission, but that the model was tightly constrained by these data.

EUV observations are perhaps the most sensitive measurement of the temperature since the EUV flux varies by more than two orders of magnitude as the surface temperature varies from 25,000 to 32,000 K. Cash, Bowyer and Lampton (1978) obtained new upper limits on the EUV flux from Sirius which were disastrous for the photospheric model. Although these results were obtained from a short observation on a rocket flight, they were considerably more sensitive than the Apollo-Soyuz results because of the use of a grazing incidence imaging telescope. With imaging the stellar flux need only stand above the average background per resolved pixel rather than above the total background flux in the field of view of the collector as was the case for the Apollo-Soyuz telescope. In this experiment the pointing was verified inflight by the observation of Sirius A with a far ultraviolet bandpass of the telescope. The pointing was confirmed postflight with pictures taken with a coaligned camera which recorded pictures of the optical field during the Sirius pointing. Since the payload was recovered, a postflight calibration was carried out; this showed no measurable change in the thin metallic film-detector combination indicating constancy to better than at least 20%. The results obtained are shown in Figure 10. These limits put a 3σ upper bound of 30,000 K on Sirius B and rule out the photospheric model for the soft X-ray flux.

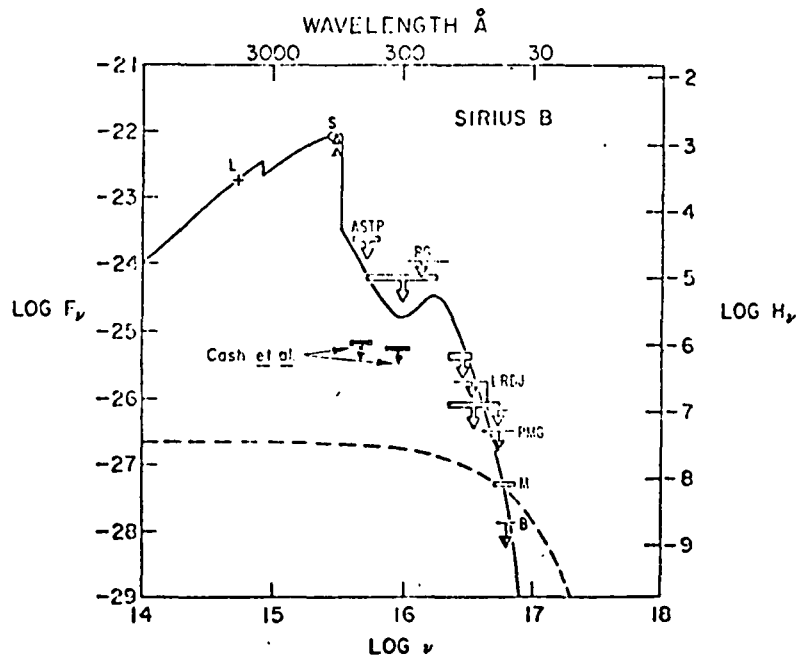


Fig. 10 - Experimental data on the spectrum of Sirius B plotted with the model atmosphere of Shipman, 1976 (solid line) and the pure bremsstrahlung corona of Lampton and Mewe, 1979 (dashed line). The 3-sigma EUV upper limits of Cash, Bowyer and Lampton, 1978, rule out a photospheric origin for the soft X-ray flux. This result is confirmed by the far UV limits of Brune, Feldman, and Mount at 1000 to 1080 Å. Their results are shown by small triangles (upper symbol: 99.3% confidence level; lower symbol: 91% confidence level). (After Cash, Bowyer and Lampton).

The results of Cash *et al.* were confirmed by a measurement of the ultraviolet spectrum of Sirius B with a rocket-borne ultraviolet spectrometer covering the wavelength band from 912 to 1240 Å (Brune *et al.*, 1978). A subset of the data obtained was used to set an upper limit on the flux from Sirius B. Data from channels below 1000 Å were not used because of a large and uncertain atmospheric absorption at these wavelengths (the absorption longward of 1000 Å averaged less than 25% and was better understood). Fluxes above 1080 Å were avoided because of possible contamination from Sirius A. A 99.3% confidence level to the 1000-1080 Å flux of 2×10^{-10} ergs $\text{cm}^2 \text{s}^{-1} \text{Å}^{-1}$ was obtained and is shown in Figure 10. A 91% confidence level upper limit to this flux, corresponding to a temperature of 27,000 K, is also shown.

Koester (1979) reanalyzed the uvby colors of Rakos and Havlen (1977) with an improved set of model atmospheres and obtained $T = 22,500$ K with a formal error of ± 600 K. As an independent alternative he combined the observed V magnitude with V band model fluxes and combined this with a radius obtained from the Hamada, Salpeter mass-radius relation. The resulting temperature was $27,400 \pm 1000$ K. Savedoff *et al.* (1978) have reported a preliminary result from an extended set of Copernicus spectra of $T \sim 27,000$ K.

As of this writing the temperature of Sirius B is not well known. Preliminary data from the HEAO-2 spacecraft (P. Charles, private communication) indicate that both Sirius A and Sirius B emit X-rays with the majority of the flux emanating from Sirius A. When viewed with the naked eye on a clear spring night, Sirius certainly doesn't seem all this puzzling.

VIII. Future Prospects

Estimates of the number density of hot white dwarfs vary widely and little direct observational evidence is available. Carnochan et al. (1975), from data obtained with the Ultraviolet Sky Survey Telescope on the TD1A satellite, have found an unexpected high density of ultraviolet-bright stars. A number of these are unexplained objects showing ultraviolet excesses inconsistent with their optical spectra (Barbier et al., 1978). Some have been identified as physical or optical pairs in which the less luminous, hot companion is a hot subdwarf (Dworetzky et al., 1977; Berger and Fringant, as quoted by Laget, 1979). A far ultraviolet objective prism survey carried out on the Spacelab missions has made similar detections; one object discovered was a hot subdwarf (Parsons et al., 1976a), but at least one was a nearby hot white dwarf which is entirely unobservable at optical wavelengths (Parsons et al., 1976b). On the other hand, Laget (1979) has carried out a balloon-borne deep (14 to 15 magnitude) ultraviolet survey covering 200 square degrees and, on the basis of his results, suggests that the density of sdO's, at least, may be comparable to that found in ground-based studies. R. Green and S. Kahn (private communication) are searching for soft X-ray emission from candidate UV excess white dwarfs from the catalogue of Green (1977). Only DO's have been examined so far and although a number of candidates with T_{eff} greater than 50,000 K exist, none were found as soft X-ray sources. These might well be EUV sources and yet not emit soft X-rays because of helium absorption shortward of 228 Å.

Henry et al. (1976) established the first upper limits on the space density of O subdwarfs and hot white dwarfs from an EUV survey over wavelengths from 135 - 475 Å, covering approximately 1350 square degrees. The upper limits obtained are shown in Figure 11. Cash, Malina and Stern (1976) used soft X-ray data from a Berkeley rocket-borne experiment to set much tighter limits on the space density of very high temperature dwarfs, and Wesemael (1978) combined data from the soft X-ray sky survey of Vanderhill et al. (1975) with detailed model calculations to obtain even more stringent limits. Their results for white dwarfs with $T \gtrsim 10^5$ K are shown in Figure 12. Even considering the uncertainties in the density of the interstellar medium and the appropriate stellar models, an upper limit of 1 to 10 very hot white dwarfs within 100 pc of the Sun has been established by these data. This limit provides a strong indication that cooling by neutrino emission is significant in hot white dwarfs.

Koester (1978) has computed the number of hot white dwarfs within 100 pc as a function of temperature. His results for two different cooling rates, one including cooling by neutrinos and one without, are shown in Figure 13. In this calculation a birthrate was assumed

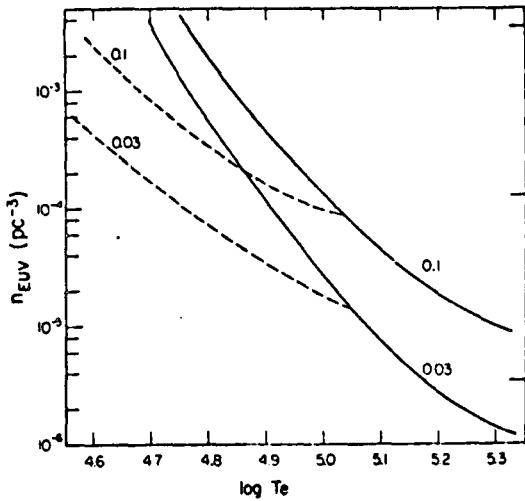


Fig. 11 - Upper limits on the space density of O subdwarfs (dotted lines) and hot white dwarfs (solid lines) as a function of effective temperature for two values of assumed interstellar neutral hydrogen density. (After Henry *et al.*, 1976).

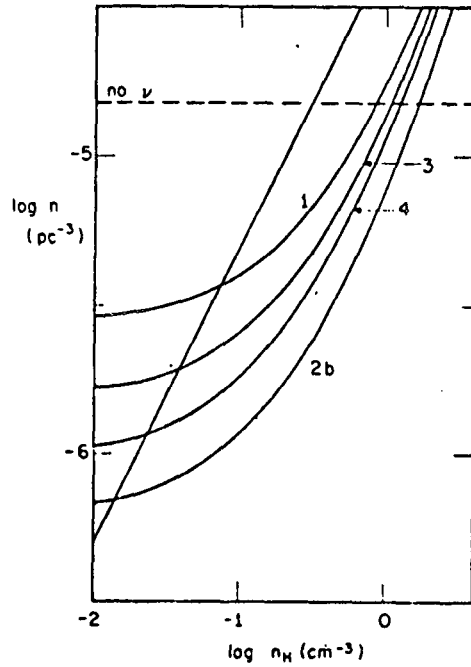


Fig. 12 - Upper limits on the number density of white dwarfs with $T \gtrsim 10^5$ K as a function of interstellar hydrogen density. The solid line refers to the upper limits of Cash *et al.*, 1976, and the curves refer to the limits of Wesemael, 1978, for differing stellar models. The theoretical estimate without neutrino cooling is shown as a dashed line. (After Wesemael, 1978).

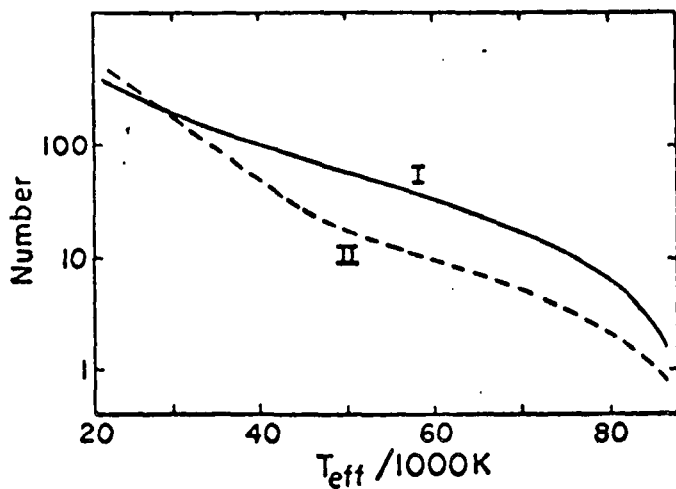


Fig. 13 - Number of white dwarfs hotter than T_{eff} within 100 pc. Curve I is without neutrino cooling and Curve II includes neutrino cooling. (After Koester, 1978)

which gave the appropriate space density for the cooler white dwarfs but in any case, only the relative numbers are important since neutrino cooling (if it actually occurs) is operative only at higher temperatures and both curves coalesce at lower temperatures. A substantial number of hot white dwarfs are predicted, which is obviously encouraging to me as an observer. More important, however, is that a determination of the relative numbers of stars as a function of temperature will help establish the role of neutrino cooling.

Muchmore and Böhm (1978) have argued that moderately hot non-DA white dwarfs (e.g., $T \sim 2 \times 10^4$ K) are likely to produce a corona as a consequence of their helium convection zone. The temperatures of these coronae will range upward to 10^6 K. These authors calculate that the flux emitted near the He II $\lambda 228$ absorption edge is of the order of 10^{12} ergs s^{-1} Hz^{-1} which, for a white dwarf at 40 pc, results in a flux at Earth about three orders of magnitude below that of HZ 43. However, given the capabilities of existing instrumentation, these sources can be readily detected if, in fact, they exist. The data on Sirius B discussed earlier certainly lend support to this hypothesis.

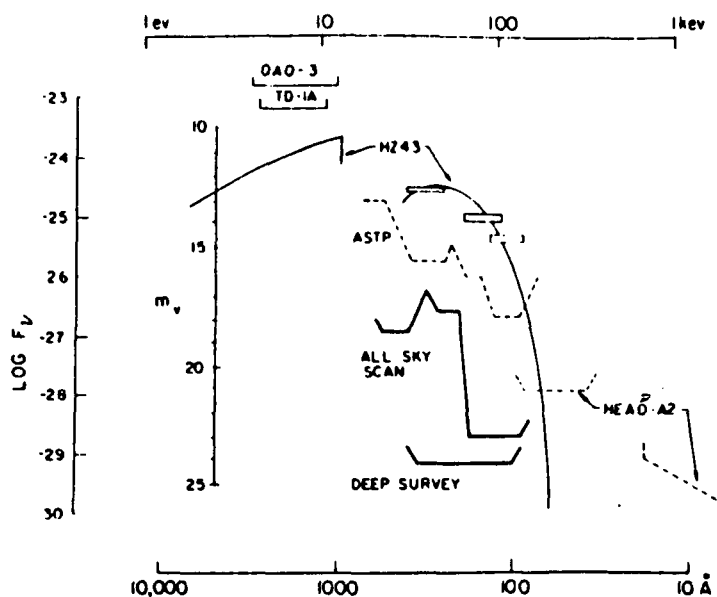


Fig. 14 - The sensitivity of the all-sky EUV survey mission approved by NASA. The heavy line marked All-Sky Scan shows the sensitivity of the survey; the heavy line marked Deep Survey is the sensitivity which will be obtained with a telescope designed to study a representative 10% of the sky.

NASA has approved an Explorer mission to carry out an EUV all-sky survey which will be significant for research in white dwarfs. The instrumentation will consist of three imaging telescopes, each with a different EUV bandpass, which will scan the sky as the spacecraft rotates. In the configuration envisaged, the sky will be surveyed in

six months. A fourth telescope mounted at right angles to these three will scan a band of the sky centered down the Earth's shadowcone, where background from the plasmosphere is at a minimum. Although only a portion of the sky will be scanned by this telescope, the sensitivity will be much higher because of the longer observing times, and because of the lower background in this region. The sensitivity of this mission, which is currently planned for launch in October of 1984, is shown in Figure 14. With the sensitivities expected, substantial numbers of white dwarfs might reasonably be expected to be found and the white dwarf coronae suggested by Muchmore and Bohm should be readily detected. Indeed, substantial ground-based observations will unquestionably be required to establish the nature of those sources discovered. It seems clear, however, that EUV observations will be of real help in developing our understanding of white dwarfs.

Acknowledgments. I would like to acknowledge the contributions, support, and encouragement of my colleagues and students at Berkeley. I would also like to acknowledge the continuous support of NASA for this work.

REFERENCES

- Auer, L., Shipman, H. 1977, *Ap. J.*, 211, L103.
- Barbier, R., Dossin, F., Jaschek, C., Jaschek, M., Klutz, M., Swings, J.P., and Vreux, J.M. 1978, *Astron. Astrophys.*, 66, L9.
- Bleeker, J.A.M., Davelaar, J., Deerenberg, A.J.M., Huizenga, H., Brinkman, A.C., Heise, J., Tanaka, Y., Hayakawa, S., and Yamashita, K. 1978, *Astron. Astrophys.* 69, 145.
- Brune, W., Feldman, P., Mount, G. 1978, *Ap. J.*, 225, L67.
- Carnochan, D., Dworetzky, M., Todd, J., Willis, A., Wilson, R. 1975, *Phil. Trans. R. Soc. Lond.*, A279, 479.
- Cash, W., Bowyer, S., Lampton, M. 1978, *Ap. J.*, 221, L87.
- _____ 1979, *Astron. Astrophys.*, (in press).
- Cash, W., Malina, R.F., Stern, R. 1976, *Ap. J.*, 204, 7.
- Cruddace, R., Paresce, F., Bowyer, S., Lampton, M. 1974, *Ap. J.*, 187, 497.
- Durisen, R., Savedoff, M., Van Horn, H. 1976, *Ap. J.*, 206, L149.
- Dworetzky, M., Lanning, H., Etzel, P., Patenande, D. 1977, *Mon. Not. Roy. Ast. Soc.*, 181, 13p.
- Eggen, O., Greenstein, J. 1965, *Ap. J.*, 141, 83.
- Fahr, J. 1974, *Space Science Rev.*, 15, 483.
- Feige, J. 1958, *Ap. J.*, 128, 267.
- Fontaine, G., Michaud, G. 1979, *Ap.J.*, (in press).
- Freeman, J., Paresce, F., Bowyer, S. 1979, *Ap. J.*, 231, L37.
- Green, R. 1977, Ph.D. Thesis, Calif. Inst. of Tech.
- Greenstein, J., Oke, J. 1979, *Ap. J.*, 229, L141.
- Greenstein, J., Oke, J., Shipman, H. 1971, *Ap. J.*, 169, 563.
- Greenstein, J., Sargent, A. 1974, *Ap. J. Suppl.*, 28, No. 259, 157.
- Hearn, A., Mewe, R. 1976, *Astron. Astrophys.*, 50, 319.
- Hearn, D., Richardson, J.A., Bradt, H.V.D., Clark, G.W., Lewin, W.H.G., Mayer, F., McClintock, J.E., Primini, F.A. and Rappaport, S.A. 1976, *Ap.J.*, 203, L21.

References cont.

- Heise, J., Huizenga, H. 1979, *Astron. Astrophys.*, (in press).
- Henry, P., Bowyer, S., Lampton, M., Paresce, F., Cruddace, R. 1976, *Ap.J.*, 205, 426.
- Holm, A. 1976, *Ap.J.*, 210, L87.
- Humason, M., Zwicky, F. 1947, *Ap.J.*, 105, 85.
- Koester, D. 1976, *Astron. Astrophys.*, 52, 415.
- _____, 1978, _____ 65, 449.
- _____, 1979, _____ 72, 376.
- Laget, M. 1979, *Astron. Astrophys.*, (in press).
- Lampton, M., Margon, B., Paresce, F., Stern, R., Bowyer, S. 1976, *Ap. J.*, 203, L71.
- Lampton, M., Mewe, R. 1979, *Astron. Astrophys.*, (in press).
- Liebert, J., Dahn, C., Gresham, M., Strittmatter, P.A. 1979, *Ap.J.*, (in press).
- Liebert, J., Margon, B. 1977, *Ap.J.*, 216, 18.
- Luyten, W. 1949, *Ap.J.*, 109, 528.
- Mack, J., Paresce, F., Bowyer, S. 1976, *Applied Optics*, 15, 861.
- Malina, R., Bowyer, S. 1979, in preparation.
- Malina, R., Bowyer, S., Finley, D., Cash, W. 1979, *SPIE*, 184, (in press).
- Malina, R., Bowyer, S., Paresce, F. 1979, *COSPAR: X-Ray Astronomy*, p. 287.
- Margon, B., Lampton, M., Bowyer, s., Stern, R., Paresce, F. 1976a, *Ap.J.*, 210, L79.
- Margon, B., Liebert, J., Gatewood, G., Lampton, M., Spinrad, H., Bowyer, S. 1976b, *Ap.J.*, 209, 525.
- Margon, B., Malina, R.F., Bowyer, S., Cruddace, R., Lampton, M. 1976c, *Ap.J.*, 203, L25.
- McKee, C. Ostriker, J. 1977, *Ap.J.*, 218, 148.
- Mewe, R. Heise, J., Gronenschild, E., Brinkman, A., Schrijver, J., den Boggende, A. 1975, *Ap.J.*, 202, L67.
- Muchmore, D., Böhm, K. 1978, *Astron. Astrophys.*, 69, 113.

References cont.

Mullan, D. 1976, Ap.J., 209, 171.

Oke, J. 1974, Ap.J. Suppl., 27, No. 236, 27.

Parsons, S., Henize, K., Wray, J., Benedict, G., Laget, M. 1976b,
Ap.J., 206, L71.

Parsons, S., Wray, J., Kondo, Y., Henize, K., Benedict, G. 1976a,
Ap.J., 203, 435.

Rakos, K., Havlen, R. 1977, Astron. Astrophys., 61, 185.

Sagdeev, R., Kurt, V., Bertaux, J. 1979, IAU Circular No. 3261.

Savedoff, M.P., Van Horn, H.M., Wesemael, F., Auer, L.H., Snow, T.P.,
and York, D.G. 1976, Ap.J., 207, L45.

Savedoff, M., Wesemael, F., Auer, L., Kerridge, S., Van Horn, H. 1978,
B.A.A.S., 10, 637.

Shipman, H. 1972, Ap.J., 177, 723.

_____, 1976, Ap.J., 206, L67.

Shipman, H., Margon, B., Bowyer, S., Lampton, M., Paresce, F., Stern,
R. 1977, Ap.J., 213, L25.

Thorstensen, J., Charles, P., Margon, B., Bowyer, S. 1978, Ap.J.,
223, 260.

Vanderhill, M., Borken, R., Bunner, A., Burstein, P., Kraushaar, W.,
1975, Ap.J., 197, L19.

Vauclair, G., Reisse, C. 1977, Astron. Astrophys., 61, 415.

Wesemael, F. 1978, Astron. Astrophys., 65, 301.

Wesselius, P., Koester, D. 1978, Astron. Astrophys., 70, 745.